Pawar *et al.*
Journal of Engineering and Applied Science (2024) 71:58
https://doi.org/10.1186/s44147-024-00395-w

Journal of Engineering and Applied Science

RESEARCH Open Access

Experimental investigation on titanium alloys for machining of stepped circular holes using ultrasonic-assisted hybrid ECM

Ashish Pawar[1*], Dinesh Kamble[2] and D. B. Jadhav[3]

*Correspondence: ashish.pawar@mitwpu.edu.in

[1] Dept. of Mech Engg. Dr. Vishwanath Karad MITWPU, Pune, India
[2] Mechanical Engineering Dept, VIIT, Pune, India
[3] Bharati Vidyapeeth Deemed to Be University College of Engineering, Pune, India

Abstract

In the recent development of high-performance gas turbine engine, there is a tendency to design the cooling holes in order to improve the heat transfer and cooling efficiency. Titanium alloy is the most preferred material for these blades. It is hard material, and hence, the traditional drilling is not appropriate for "Ti" alloy. This research presents the design and optimization required to manufacture contoured holes on a titanium-based superalloy using hybrid electrochemical machining (ECM) under different operating conditions. The circular holes are developed and are analyzed by ANOVA. The experimental results are further optimized using a Technique for Order of Preference by Similarity to Ideal Solution (TOPSIS) method. The voltage (*V*), feed rate (f_1), and feed rate (f_2) were identified as the most influencing factors which are further used for stepped circular hole machining. A design of the experiment is also optimized using the TOPSIS method. The obtained experimental results are verified using a SEM analysis to confirm the uniformity of the machined surfaces and the inverse relationship of the overcut with the increasing values of the voltages and feed rates. Optimal machining conditions for the stepped hole machining were determined for voltage 18 V, feed rate "f_1" at 0.8 mm/min, and feed rate "f_2" at 1.35 mm/min.

Keywords: Contoured holes, ANOVA, TOPSIS, SEM, Voltage, Feed rate, Tool profiles

Springer Open

© The Author(s) 2024. **Open Access** This article is licensed under a Creative Commons Attribution 4.0 International License, which permits use, sharing, adaptation, distribution and reproduction in any medium or format, as long as you give appropriate credit to the original author(s) and the source, provide a link to the Creative Commons licence, and indicate if changes were made. The images or other third party material in this article are included in the article's Creative Commons licence, unless indicated otherwise in a credit line to the material. If material is not included in the article's Creative Commons licence and your intended use is not permitted by statutory regulation or exceeds the permitted use, you will need to obtain permission directly from the copyright holder. To view a copy of this licence, visit http://creativecommons.org/licenses/by/4.0/. The Creative Commons Public Domain Dedication waiver (http://creativecommons.org/publicdomain/zero/1.0/) applies to the data made available in this article, unless otherwise stated in a credit line to the data.

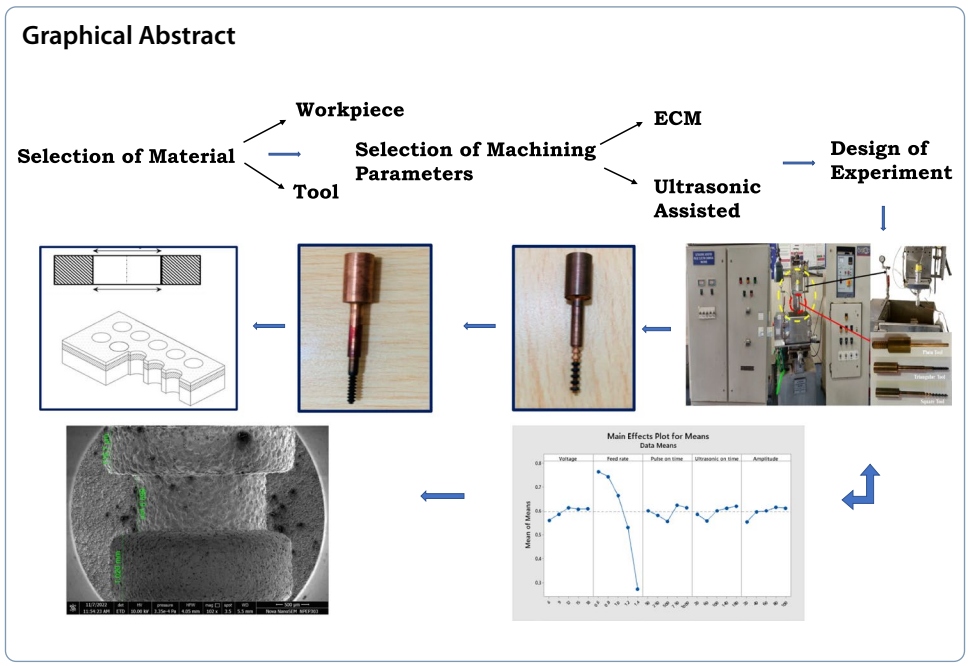

Introduction

The input temperatures of gas turbines are observed with higher values over the period of time on account of a regular improvement in the efficiency and higher firing temperatures. In the 1960s, the properties of the materials used limited the temperature of gas turbine firing and the temperature of turbine blades to approximately 800 °C. To achieve maximum power output and thermal efficiency, modern gas turbine engines operate at temperatures ranging from 1200 to 1500 °C. The failure of thermal insulation of the blade is observed due to the rising temperature of the gas and a transfer of heat to it. The temperatures observed in the first stage of todays modern gas turbine engines and its surroundings are significantly high. High-pressure stage airfoils need to be cooled in order to keep their structural integrity. These cooling techniques typically consist of internal passages of varying shapes [1]. Film cooling is a method that is well accepted and frequently used in modern gas turbine cooling system to maintain the surface temperatures of components within acceptable limits. To ensure the safe operation of the engine blade, both external and internal cooling methods have been selected. By injecting cool air from the inside of the blade to the outside surface, external cooling is achieved, and a film layer forms between the blade surface and hot gas-pass flow. The shaped hole film-cooling technology is now standard in highly cooled gas turbine aerofoils. It is common practice to distribute the ribs on the wall of an inlet cooling hole in order to enhance the heat transfer rate. It is also known as turbulators. A thermal barrier is created by these ducts between the blade and the hot gases that are flowing through the main flow path of the engines. The increased contact surface between the metal and the cooling air along with a heat exchange due to turbulence contributes to the enhancement of the effectiveness of these holes in the cooling process [2].

In general, a turbine blade could have several hundred film-cooling holes, each of which is between 0.2 and 0.8 mm in diameter [2, 3]. Titanium is widely used in turbine blades due to its excellent combination of properties such as high strength, low density, and good corrosion resistance. The use of titanium in turbine blades has been

extensively studied and documented in the literature. The manufacturing of micro holes in titanium-based super alloys can be challenging due to the material's unique properties. Titanium-based super alloys are also very hard, which can make them difficult to machine. The high hardness of the material can cause excessive tool wear, which leads to a shorter tool life and increased manufacturing costs. It is also reactive with material like cutting tools and coolants. To address these issues, manufacturers may use specialized machining techniques, cutting tools, and coolants that are designed specifically for titanium-based super alloys [4, 5]. Micro electrical discharge machining (micro EDM), laser beam machining, and ultrasonic machining are the three methods that have been utilized to create micro holes. Micro EDM and laser beam machining are both thermal manufacturing processes, and hence, the machined workpiece shows heat-affected zones as well as micro cracks. Ultrasonic milling presents a few challenges, including increased tool wear and a heightened sensitivity to variations in material strength. Electrochemical machining techniques, on the other hand, do not leave any heat-affected layers and do not cause tool wear because ECM involves an anodic electrochemical dissolution process in an electrolyte.

ECM is frequently utilized in the machining of hard alloys because it is capable of removing electrically conductive materials irrespective of their hardness and toughness [5, 6]. The absence of metal cutting forces, micro cracks, and a good surface quality makes an ECM process as a mainstream manufacturing technology for a part with complex structures in aeroengines [7–9]. The ECM is further advanced as hybrid ECM and ultrasonic-assisted ECM.

The ECM process involves the controlled anodic electrochemical dissolution of components in an electrolytic cell [10]. The ECM process has certain features, such as a high rate of material removal and no wear on the tools. It provides a good surface quality without the occurrence of re-solidified layers, heat-affected zone, and strain hardening [11]. The complexity of profile and coupling of multiple physical fields lead to difficulty in removing material from the interelectrode gap. Klocke et al. [12, 13] developed an interdisciplinary model to simulate the ECM process for aero-engine blades. It is reported that the suitable cathode geometries can be calculated directly in a virtual design step by using inverse simulation. The external cooling methods are studied by Sargison et al. [14]. They present flow visualization experiments for a new film-cooling hole called the converging slot hole or console, which has been shown to improve heat transfer and aerodynamic performance in turbine vane and rotor blade cooling systems. Results showed that the console film was similar to a slot film and remained thin and attached to the surface for certain coolant-to-mainstream momentum flux ratios. Gritsch et al. [15] presents measurements of local heat transfer coefficients in the vicinity of three film-cooling holes with different geometries. Results showed that expanded holes had lower heat transfer coefficients than the cylindrical hole, particularly at high blowing ratios, and the laidback fan-shaped hole provided better lateral spreading of the injected coolant. The superposition method was applied to evaluate the overall film-cooling performance of the hole geometries. Garg [16] presented external flow, and heat transfer characteristics over smooth and rough turbine blades for a range of parameter values are described, as well as the effect of film-cooling holes and internal cooling channels with ribs and bleed holes on smooth blades. Several studies on the blade tip region, susceptible to burnout

and oxidation, are also described. Han and Dutta [17] in his research on the internal cooling methods has reported. This paper provides a review of recent developments in turbine blade internal cooling, with a focus on the use of rib-enhanced serpentine passages, jet impingement. The machining debris of zirconia is examined by He et al. [18] using Raman spectroscopy during spark-assisted chemical engraving. It is concluded that due to differences in phase composition, the material removal is influenced by physical and chemical phenomena in 75.8% and 24.2%, respectively. Gruner et al. [19] studied hole drilling on stainless steel using a high repetition frequency femtosecond laser (220 fs and 1030 nm). This research determines the optimal parameters for the highest available drilling quality and speed.

Burger et al. [20] found that the ECM reduces the cost of manufacturing a single blade by 30% in batch production due to reduced tooling costs. Zhang et al. [21] advocated for precision drilling with an ultrashort pulse laser (such as picosecond and femtosecond) to improve the quality of holes, and they demonstrated that picosecond laser helical drilling can manufacture high-quality holes with a significantly reduced recast layer thickness (less than 5 μm). Liu et al. [22] developed a modified tool to eliminate overcut in ECM of repaired turbine blade tips and obtained an optimal machining time with an appropriate voltage. They did this by obtaining an optimal machining voltage. After using a millisecond laser and a femtosecond laser in a two-step process, Wang et al. [23] finally succeeded in producing high-quality holes in thermal barrier-coated nickel-based alloys. Romoli et al. [24] designed a micro-drilling cycle that used ultrashort laser pulses and was based on three phases in sequence: drilling through, enlarging, and finishing. These authors showed that this drilling strategy was able to produce cylindrical holes with diameters of 180 ± 2 μm on a plate that was 350 μm thick with the complete absence of burrs and debris. Jain et al. [25] proposed analytical equation techniques in order to predict stepped holes and most significant parameters. These models were used to predict and analyze the behavior of the workpiece. Reddy et al. [26] developed a tool design model that is based on the use of a correction factor method to repeatedly modify the shape of the tool until an anode profile is obtained that is within the prescribed tolerance limits. Dutta and Sarma [27] examines how input process parameters like capacitance, gap voltage, and pulse on time (ton) affect response variables like material removal rate (MRR), tool wear rate (TWR), and diametral overcut (DOC) during μ-EDM of Hastelloy C276. RSM-DF optimizes capacitance, gap voltage, and ton for maximum MRR, minimum TWR, and DOC. MOGA shows that at 1001.610 pF, gap voltage of 137.6671 V, and ton of 48.025 μs, MRR is 0.005153 mm^3/min, TWR is 0.002423, and DOC is 0.028691 mm. Pawar et al. [28–30] presented research work carried out on super alloys by researchers in the area of ECM, EMM, STEM, hybrid ECM, etc., for a wide range of super alloys and metals to advanced alloys.

From the literature review, it is seen that the machining of titanium alloy using ECM plays an important role which overcomes the difficulties and complexity arising during the machining. The productivity of the ECM process can be further improved by using a hybrid approach like the use of ultrasonic pulses, abrasive, and laser. From the review of the literature, it is also clear that stepped hole machining of titanium alloy using hybrid ECM needs more attention because it needs to be done with the best machining parameters to get better hole profiles. The multi-criteria decision-making technique has various

methods which are found to be useful in multi-objective optimization. Many researchers use the TOPSIS method to solve their multi-objective optimization problems, which shows how important the TOPSIS method is in the multi-objective optimization domain [31]. TOPSIS (Technique for Order Preference by Similarity to Ideal Solution) is a decision-making method that evaluates and ranks alternatives based on their proximity to the ideal solution and distance from the worst solution. It uses the concept of similarity to determine the best alternative among a set of options. TOPSIS involves creating a normalized decision matrix, determining the ideal and worst solutions, calculating the similarity and dissimilarity scores, and then ranking the alternatives accordingly.

The purpose of this research is to use ultrasonic-assisted ECM to identify the ideal machining conditions for plane circular holes and stepped circular holes. Under various operation conditions, two different steeped hole profiles, namely circular and stepped circular, have been produced. In this work, the impact of several factors, including voltage, feed rate, pulse on time, on material removal rate, overcut, and surface roughness, is investigated. Two phases were taken in the research process for this project. First, a circular hole was optimized multi-objectively by identifying the most significant components using ANOVA and TOPSIS. The factors that have been established are updated further for the stepped hole machining through screening trials. The remaining half of this paper describes how the TOPSIS method was used to optimize the stepped hole machining process after the indicated parameters were further studied. As a result, this study evaluates the TOPSIS method's applicability in various settings. The experimental approach of hybrid ECM, ANOVA, and TOPSIS analysis for both flat and stepped hole machining is explained in the remaining section of this study.

Experimental

The experiments are conducted on the ultrasonic-assisted pulse electrochemical machine (USAPECM). It is a nontraditional machining process that combines electrochemical machining (ECM) with ultrasonic vibration. It is used to machine complex shapes in conductive materials such as metals, alloys, and composites. The experimental setup consists of power supply, a tool electrode (anode), a workpiece (cathode), an electrolyte solution, and an ultrasonic transducer. The tool electrode is made of a conductive material and is shaped to the desired geometry of the part to be machined. The workpiece is clamped onto a fixture and submerged in the electrolyte solution. The ultrasonic transducer generates high-frequency mechanical vibrations that are transmitted to the electrolyte solution and the workpiece, as illustrated in the Fig. 1a. The photograph of different tools used and hybrid ECM is shown in Fig. 1b. These vibrations help to enhance the machining process by improving the electrolyte flow, increasing the rate of material removal, and reducing the formation of surface defects. The power supply generates the DC current to electrochemically machine the workpiece. The tool electrode and workpiece are submerged in an electrolyte solution that reacts with the workpiece material to remove material from the workpiece. The potential difference between the workpiece and the tool electrode was provided by a pulse generator.

The ECM tool electrode plays a critical role in achieving high precision and accuracy during the machining process. ECM tool electrode is a small electrically conductive tool. It is made of a conductive material copper. It is designed for a shape

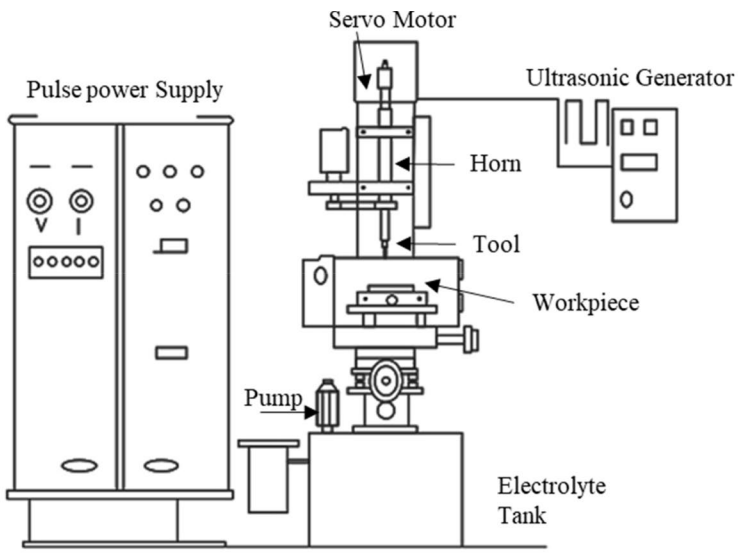

(a) Schematic of Hybrid ECM

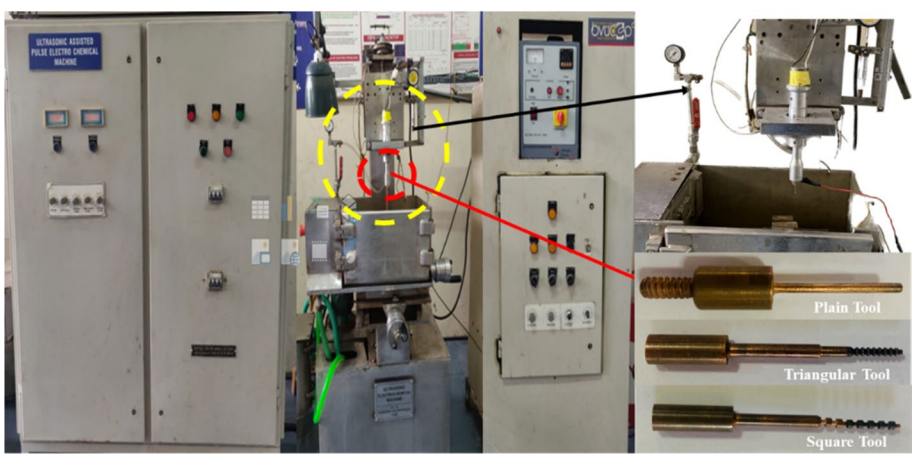

(b) Experimental Setup of Hybrid ECM

Fig. 1 **a** Schematic of hybrid ECM. **b** Experimental setup of hybrid ECM

that can be used to machine complex and intricate hole profiles (circular, rectangular, and triangular). A tool electrode of the desired shape is fabricated using wire electrical discharge machining (Fig. 2). In EDM, sequential spark discharge occurs between the tool and the workpiece. The measurement of the electrode tool is 158-mm length and 2-mm inner diameter, and 3-mm outer diameter was used as the circular tool. Similarly, the measurement of the rectangular and triangular electrode tool is 158-mm length and 2-mm inner diameter, and 3-mm outer diameter is used. The sodium chloride (NaCl) and 5% HCl having the conductivity of about 120 mS/cm is used for the machining purpose.

Ti-6–6-2 is selected as the material for the workpiece due to its high strength-to-weight ratio as requirement for turbine blade stators of aeroengines. The chemical

(a) circular (b) square (c) triangular

Fig. 2 Electrode **a** circular, **b** square, and **c** triangular for machining stepped holes

Table 1 Chemical composition of Ti-6–6-2

Material	Wt.% of composition
Titanium (Ti)	89.065
Vanadium(V)	6.423
Tin (Sn)	2.80–3.30
Iron (Fe)	0.988
Copper (Cu)	0.597
Palladium (Pd)	0.028
Molybdenum ((Mo)	0.012

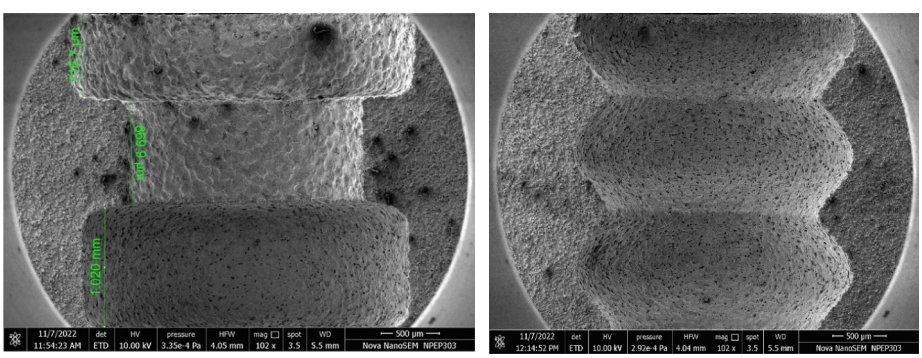

(a) SEM of square hole profile. (b) SEM of triangular hole profile.

Fig. 3 SEM images of stepped hole for **a** square profile and **b** triangular profile

compositions of material Ti-6–6-2 are given in Table 1. The specifications of a titanium alloy workpiece for machining-shaped hole are shown in Fig. 3. The thickness of the workpiece is selected 10 mm, and diameter is 3 mm.

In the ECM process, the electrolyte performs three functions: it transmits current between the tool and the workpiece, eliminates reaction products from the IEG, and removes heat created by current passage [3, 29]. In order to maintain the proper MRR, the electrolyte must be pumped through the IEG at a very high pressure. It is also important to pump the electrolyte through the IEG at a very high pressure in order to maintain

a consistent MRR [11]. The material removal rate (MRR) is determined by measuring the initial weight of the workpiece and subtracting the final weight after machining. This difference in weight is then divided by the time taken for the machining process. Using a weighing machine, this straightforward calculation provides a quantitative measure of the efficiency and speed at which material is being removed during the manufacturing or machining operation. Overcut, in electrochemical machining (ECM), refers to the variance between the size of the electrode and the cavity or hole being machined. This discrepancy is a critical parameter in ensuring precision and accuracy during the ECM process. The measurement of overcut is effectively carried out using the SIPCON vision measuring system. The stylus-type surface tester MITUTOYO make is employed to measure the surface roughness of holes machined using hybrid electrochemical machining (ECM). This specialized device utilizes a stylus or probe to traverse the contours of the machined surface, capturing detailed height variations.

Design of experiments and optimization using TOPSIS

Taguchi methods involve the use of orthogonal arrays to determine the most important factors affecting a process. These factors can be optimized. The parameters and their respective levels for machining of the circular micro holes are mentioned in Table 2. The DoE output response table for three different outputs for plain circular holes is given in Table 3. Total five parameters and five levels are considered for the analysis. The *L25* orthogonal array is a specific type of design matrix that consists of 25 experimental runs, each of which represents a unique combination of the experimental factors being tested. A separate analysis is performed for the material removal rate (MRR), overcut, and surface roughness.

The Technique for Order Preference by Similarity to Ideal Solution (TOPSIS) is a multi-criteria decision-making method that can be used to evaluate the performance of different process parameters in the fabrication of micro holes using electrochemical machining (ECM). The parametric design for the machining of titanium alloy involves the monitoring of four parameters such as voltage, micro-tool feed rate, and pulse on time.

By conducting trials with the workpiece and assuming that certain actual parameter values from earlier research efforts will be used, a general concept of the range of values to use in each level of output parameters such as MRR, overcut, and surface finish selected using the TOPSIS method rank for the circular hole as shown in Table 4.

Table 4 shows that the rank is given to experimental run 22. This is because, according to the TOPSIS analysis, all three output responses are equally important, so each one

Table 2 Parameters and the levels of USAPECM

Sr. no	Parameter	Unit	Level 1	Level 2	Level 3	Level 4	Level 5
1	Feed rate	mm/min	0.6	0.8	1	1.2	1.4
2	Voltage	V	6	9	12	15	18
3	Pulse on time	μs	50	250	500	750	1000
4	Ultrasonic on time	s	20	60	100	140	180
5	Amplitude		20	40	60	80	100

Table 3 Taguchi DoE with output responses for plain circular hole

Exp. run	Voltage	Feed rate	Pulse on time	Ultrasonic on time	Amplitude	MRR (g/min)	Overcut (mm)	Surface roughness (micrometer)
1	6	0.6	50	20	20	0.004023	1.25	1.146
2	6	0.8	250	60	40	0.004223	1.43	1.326
3	6	1	500	100	60	0.004473	1.58	1.477
4	6	1.2	750	140	80	0.004573	1.68	1.577
5	6	1.4	1000	180	100	0.004598	2.19	2.088
6	9	0.6	250	100	80	0.004773	1.3	1.196
7	9	0.8	500	140	100	0.005023	1.44	1.336
8	9	1	750	180	20	0.005123	1.6	1.497
9	9	1.2	1000	20	40	0.005123	1.8	1.697
10	9	1.4	50	60	60	0.005224	2.3	2.198
11	12	0.6	500	180	40	0.005224	1.31	1.206
12	12	0.8	750	20	60	0.005424	1.46	1.356
13	12	1	1000	60	80	0.005474	1.62	1.517
14	12	1.2	50	100	100	0.005474	1.8	1.697
15	12	1.4	250	140	20	0.005474	2.32	2.218
16	15	0.6	750	60	100	0.005474	1.36	1.256
17	15	0.8	1000	100	20	0.005524	1.49	1.386
18	15	1	50	140	40	0.005524	1.64	1.537
19	15	1.2	250	180	60	0.005624	1.84	1.737
20	15	1.4	500	20	80	0.005724	2.43	2.328
21	18	0.6	1000	140	60	0.005924	1.39	1.396
22	18	0.8	50	180	80	0.006024	1.5	1.286
23	18	1	250	20	100	0.006024	1.67	1.567
24	18	1.2	500	60	20	0.006224	2.18	2.078
25	18	1.4	750	100	40	0.006724	2.56	2.458

was given the same weight of 0.33. The best combinations of the experimental runs using the TOPSIS method were identified as 22–21-16–11-12–17-6–7-23–1-13–18-8–2-3–4-14–19-9–24-25–5-15–10-20. For this experimental run 22, the factor combinations are voltage at 18 V, feed rate at 0.8 mm/min, pulse on time at 50 µs, ultrasonic on time at 180 s, and the amplitude at 80 µ.

Analysis for stepped circular hole machining

Based on a circular hole investigation followed by a screening experiment, it was seen that the voltage and two feed rates are the most responsible factors to generate the desired stepped hole profiles which were further used for investigation. The following mathematical relation was assumed to figure out two feed rates and their levels. For a stepped circular hole, the relationship between the outer diameter and the inner diameter is defined as the following:

$$Outerdiameter = 1.5 \times inputdiameter$$

It is observed from the experimental study that to generate the outer diameter and inner diameter, two feed rates are responsible which are again defined by equation [25].

Table 4 TOPSIS analysis of the plain circular hole

Exp. run	Weighted normalized matrix			Euclidean distances			
	MRR (g/min)	Overcut (mm)	Surface roughness (μm)	Si +	Si −	Relative closeness (Pi)	Rank
1	0.04956	0.04671	0.04539	0.03328	0.07141	0.6821	10
2	0.05203	0.05343	0.05255	0.03234	0.06164	0.6559	14
3	0.05511	0.05904	0.05851	0.03306	0.05370	0.6189	15
4	0.05634	0.06277	0.06248	0.03539	0.04844	0.5778	16
5	0.05665	0.08183	0.08271	0.05756	0.02137	0.2708	22
6	0.05880	0.04858	0.04738	0.02419	0.06930	0.7413	7
7	0.06188	0.05381	0.05294	0.02338	0.06228	0.7271	8
8	0.06311	0.05979	0.05930	0.02745	0.05405	0.6632	13
9	0.06311	0.06726	0.06724	0.03590	0.04358	0.5483	19
10	0.06436	0.08594	0.08708	0.06015	0.02048	0.2540	24
11	0.06436	0.04895	0.04778	0.01877	0.06973	0.7879	4
12	0.06682	0.05455	0.05374	0.01969	0.06239	0.7601	5
13	0.06744	0.06053	0.06009	0.02539	0.05426	0.6813	11
14	0.06744	0.06726	0.06724	0.03372	0.04511	0.5723	17
15	0.06744	0.08669	0.08787	0.06033	0.02215	0.2685	23
16	0.06744	0.05082	0.04977	0.01653	0.06781	0.8040	3
17	0.06806	0.05568	0.05493	0.01975	0.06118	0.7560	6
18	0.06806	0.06128	0.06089	0.02590	0.05344	0.6735	12
19	0.06929	0.06875	0.06883	0.03491	0.04392	0.5571	18
20	0.07052	0.09080	0.09223	0.06550	0.02212	0.2525	25
21	0.07298	0.05194	0.05533	0.01494	0.06503	0.8132	2
22	0.07422	0.05605	0.05096	0.01388	0.06582	0.8259	1
23	0.07422	0.06240	0.06208	0.02448	0.05441	0.6897	9
24	0.07668	0.08146	0.08232	0.05108	0.03412	0.4005	20
25	0.08284	0.09566	0.09739	0.07141	0.03328	0.3179	21

Table 5 Factors with their levels for stepped circular hole machining

Sr. no	Voltage	Feed rate (f1)	Feed rate (f2)
1	17	0.7	1
2	18	0.8	1.2
3	19	0.9	1.35

Therefore, from the Taguchi analysis of the TOPSIS and from the experimental study, the determined input factor combinations are shown in Table 5.

In Table 5, the feed rate "f1" is responsible for the outer diameter, while the feed rate "f2" is responsible for the inner diameter. From Table 5, the new design of the experiment using the Taguchi method was used for the machining of the stepped circular hole which has nine experimental runs shown in Table 6.

For stepped circular hole machining, TOPSIS analysis was performed to identify the best experimental run which is shown in Table 7.

Each of the three output responses was given the same weight of 0.33 because they were all just as important. Using the TOPSIS method, the best combinations of the test

Table 6 Taguchi DoE with output responses for the stepped circular hole machining

Exp. run	Voltage	Feed rate f1	Feed rate f2	MRR g/min	Overcut, mm	Surface roughness, mm
1	17	0.7	1	0.00562	2.61	1.282
2	17	0.8	1.2	0.00592	2.46	1.434
3	17	0.9	1.35	0.00612	2.08	1.975
4	18	0.7	1.2	0.00542	1.57	1.292
5	18	0.8	1.35	0.00582	1.54	1.182
6	18	0.9	1	0.00663	1.4	2.411
7	19	0.7	1.35	0.00537	1.39	1.152
8	19	0.8	1	0.00602	1.29	1.464
9	19	0.9	1.2	0.00642	1.26	2.356

Table 7 TOPSIS analysis for a stepped circular hole

Exp. run	Weighted normalized matrix			Euclidean distances			
	MRR (g/min)	Overcut (mm)	Surface roughness (micrometer)	Si +	Si −	Relative closeness (Pi)	Rank
1	0.06927	0.09752	0.05079	0.05221	0.04484	0.4620	7
2	0.07296	0.09192	0.05682	0.04704	0.03970	0.4577	8
3	0.07543	0.07772	0.07825	0.04519	0.02786	0.3814	9
4	0.06680	0.05866	0.05119	0.01970	0.05896	0.7496	4
5	0.07174	0.05754	0.04683	0.01452	0.06325	0.8133	1
6	0.08173	0.05231	0.09553	0.05016	0.04782	0.4880	6
7	0.06617	0.05194	0.04564	0.01630	0.06758	0.8057	3
8	0.07420	0.04820	0.05801	0.01452	0.06249	0.8115	2
9	0.07913	0.04708	0.09335	0.04778	0.05213	0.5218	5

runs for the stepped circular hole were found to be 5–8-7–4-9–6-1–2-3. In Table 7, the rank is given to the experimental run 5. For this experiment, the factor combinations are 18 V, 0.8 mm/min for "f1" feed rate, and 1.35 mm/min for "f2" feed rate. These combinations were thought to be the best ones to start with, and the Taguchi analysis was used to find out more about them.

Results and discussion

A Taguchi design experiment was conducted to assess the influence of five input variables on three output responses: Material Removal Rate (MRR), overcut, and surface finish. The primary objective of the TOPSIS method is to identify the experimental run with the highest performance relative to the others that were considered as an initial input parameter. To comprehend the importance of these input variables, an analysis of variance (ANOVA) was conducted, as shown in Table 8.

In ANOVA analysis, the input factor having *P*-value less than 0.05 is considered a significant value. The ANOVA analysis reveals that the voltage is the significant factor with a percentage contribution of 90% for MRR, 4.31% for overcut, and 4.31% for surface roughness. Additionally, the feed rate is a significant input factor with a

Table 8 ANOVA for the plain circular hole machining

Source	DF	Adj SS	Adj MS	*F*-value	*p*-value	Percentage contribution (%)
MRR						
Voltage	4	0.000009	0.000002	470.82	0.000	90.00
Feed rate	4	0.000001	0	32.05	0.003	10.00
Pulse on time	4	0	0	9.15	0.027	0.00
Ultrasonic on time	4	0	0	2.35	0.214	0.00
Amplitude	4	0	0	1.13	0.453	0.00
Error	4	0	0			
Total	24	0.00001				
R-square = 99.81%, R-square (adjusted) = 98.84%						
Overcut						
Voltage	4	0.15326	0.038314	12.03	0.017	4.31
Feed rate	4	3.31294	0.828234	260.12	0.000	93.20
Pulse on time	4	0.02822	0.007054	2.22	0.230	0.79
Ultrasonic on time	4	0.02794	0.006984	2.19	0.233	0.79
Amplitude	4	0.01974	0.004934	1.55	0.341	0.56
Error	4	0.01274	0.003184			
Total	24	3.55482				
R-square = 99.64%, R-square (adjusted) = 97.85%						
Surface roughness						
Voltage	4	0.15377	0.038443	7.12	0.042	4.31
Feed rate	4	3.29804	0.824509	152.68	0.000	92.46
Pulse on time	4	0.03315	0.008288	1.53	0.344	0.93
Ultrasonic on time	4	0.0342	0.008549	1.58	0.334	0.96
Amplitude	4	0.02641	0.006602	1.22	0.425	0.74
Error	4	0.0216	0.0054			
Total	24	3.56717				
R-square = 99.39%, R-square (adjusted) = 96.37%						
Relative closeness of TOPSIS						
Voltage	4	0.009832	0.002458	1.48	0.358	1.12
Feed rate	4	0.82251	0.205628	123.44	0.000	93.76
Pulse on time	4	0.014219	0.003555	2.13	0.24	1.62
Ultrasonic on time	4	0.01178	0.002945	1.77	0.297	1.34
Amplitude	4	0.012259	0.003065	1.84	0.285	1.40
Error	4	0.006663	0.001666			
Total	24	0.877264				
R-square = 99.24%, R-square(adjusted) = 95.44%						

percentage contribution of 10% for MRR, 93.20% for overcut, and 92.46% for surface roughness. The pulse on time is found to be the least significant factor having a percentage contribution of 0% for MRR, 0.79% for overcut, and 0.93% for surface roughness. For the TOPSIS method, the feed rate is found to be the most significant factor with a percentage contribution of 93.76% followed by pulse on time at 1.62% and voltage with the least significant of 1.12%. The Taguchi analysis of the TOPSIS method for the plain circular hole was performed. The main effect plot for means of the TOPSIS method is shown in Fig. 4. From Fig. 4., final optimal machining conditions are identified as the voltage at 12 V, feed rate at 0.6 mm/min, pulse on time at

a. Main Effect plot for Stepped Hole Profiles

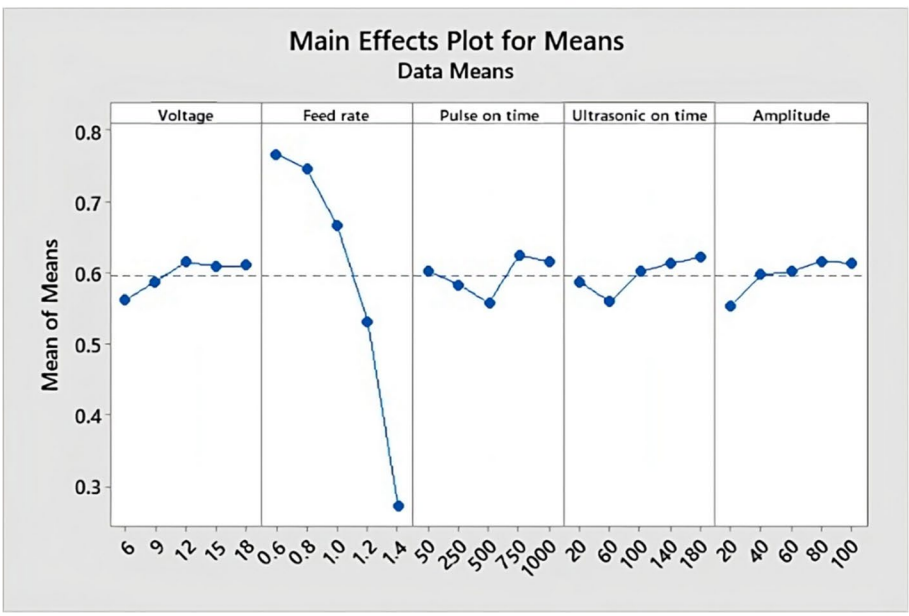

b. Main effect plots of TOPSIS method for the plane circular hole.

Fig. 4 **a** Main effect plot for stepped hole profiles. **b** Main effect plots of TOPSIS method for the plane circular hole

750 µs, ultrasonic on time at 180 s, and the amplitude at 80 µ. For these conditions, confirmation experiment was performed, and the result of the confirmation experiment is shown in Table 7. The design of experiments (DoE) for stepped circular hole machining primarily focuses on the analysis of voltage and feed rates using ANOVA.

Table 9 Confirmation experiment for the plain circular hole

	Initial parameter conditions (from TOPSIS ranking — expt. run = 22)	Optimal parameter conditions (from Taguchi analysis of TOPSIS method)	Percentage improvement (%)	Remark
	A5B2C1D5E4	A3B1C4D5E4		
MRR	0.006024	0.004123	46.10720349	Negative
Overcut	1.5	1.4	7.142857143	Positive
Surface roughness	1.286	1.326	3.100944359	Negative
	Overall improvement		42.06529071	Negative

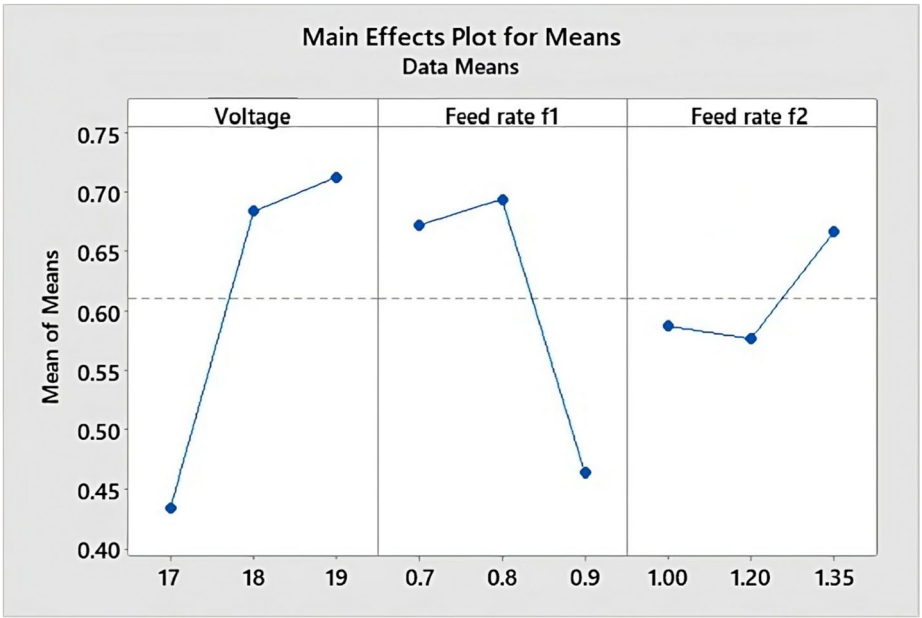

Fig. 5 Main effect plot of the TOPSIS method for a stepped circular hole

The MRR is improved by 46.10%, overcut is reduced by 7.14%, and surface roughness is increased by 3.10% as per Table 7. Thus, overall, the performance of the Taguchi analysis is reduced by 42.06% (Table 9). Hence, the final optimal conditions for plain circular hole machining are confirmed as the same conditions determined by the TOPSIS method. For the stepped hole machining, voltage (v), feed rate (f_1), and feed rate (f_2) are chosen as input factors. The ANOVA analysis results clearly highlight the significance of these three factors. Similar to the Taguchi analysis of the TOPSIS method for the plane circular hole, the Taguchi analysis of the TOPSIS method for the stepped circular hole is also performed (Fig. 5). It is observed that the optimal machining conditions are identified as the voltage at 19 V, feed rate "f_1" at 0.8 mm/min, and feed rate "f_2" at 1.35 mm/min.

The confirmation experiment for the optimal machining conditions determined by the Taguchi analysis of the TOPSIS method for the stepped circular hole was performed. The results of the confirmation experiment are shown in Table 10.

The MRR is improved by 6.71%, overcut is reduced by 40.26%, and surface roughness is increased by 53.30% as per the results shown in Table 10. Thus, overall

Table 10 Confirmation experiment for the stepped circular hole

	Initial parameter conditions (from TOPSIS ranking — expt. run = 5)	Optimal parameter conditions (from Taguchi analysis of TOPSIS)	Percentage improvement (%)	Remark
	A2B2C3	A3B2C3		
MRR	0.005823	0.006214	6.714751846	Positive
Overcut	1.54	2.16	40.25974026	Negative
Surface roughness	1.182	1.812	53.29949239	Negative
	Overall improvement		86.8444808	Negative

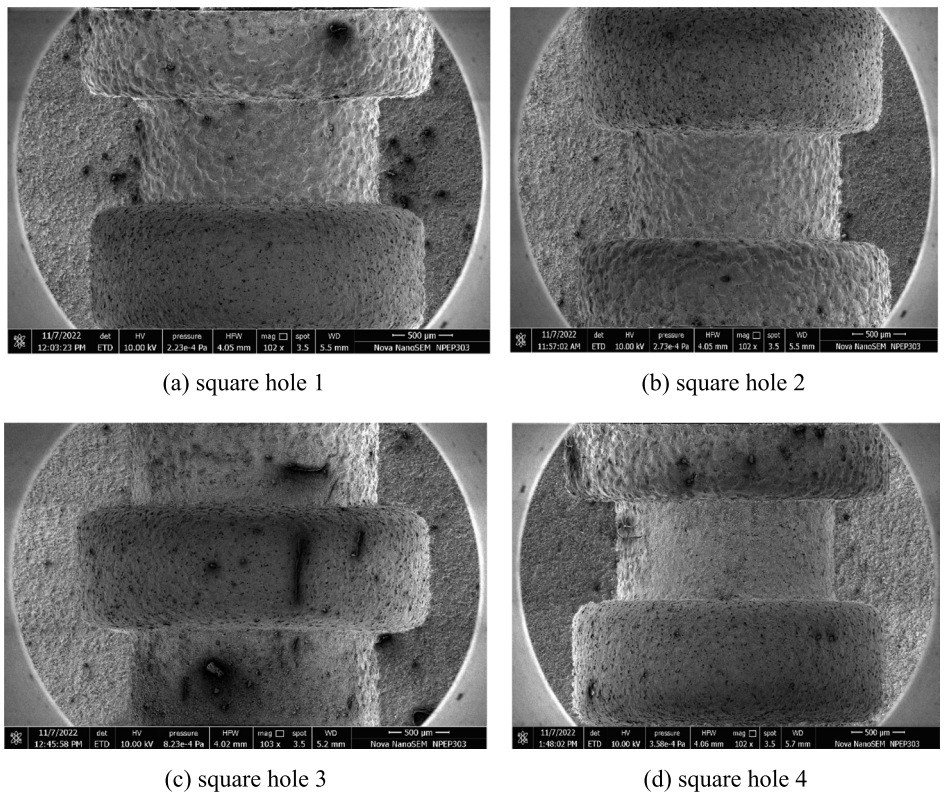

Fig. 6 SEM images for square hole. **a** Square hole 1. **b** Square hole 2. **c** Square hole 3. **d** Square hole 4

performance is reduced by 86.84%. Therefore, the optimal machining conditions for the stepped circular hole were confirmed to be the same as those determined by the TOPSIS method.

The SEM images presented in Fig. 6 illustrate the results from various experimental runs involving stepped circular holes. These images provide clear evidence that the profiles of the stepped holes were exclusively influenced by the voltage and feed rates (f1 and f2), all of which yielded distinct output response values. This observation serves to validate and affirm the accuracy of both the ANOVA analysis and the TOPSIS method employed for plain circular hole assessment, establishing their applicability in determining the optimal input parameters for stepped circular hole machining.

Morphology of square hole and surface analysis

Figure 7 shows a SEM image of the stepped circular hole. The voltage (V), feed rate (f_1), and feed rate (f_2) have a uniform effect on the stepped hole profile. The SEM analysis also shows that there is no generation of the built-up edge formation. This reveals that the chip and bur produced during the machining are removed efficiently by the electrolyte. Also, at the same time, the electrolyte helps to reduce the rubbing action of the bur over the surface. The SEM image reveals that the voltage (V), feed rate (f1), and feed rate (f2) have a uniform effect on the profile of the stepped hole. This suggests that the changes in these parameters have consistent and predictable impacts on the machining results. The efficient chip removal prevents accumulation and interference, contributing to a smoother and more precise machining process. As a result, the ECM achieves a superior surface finish with uniform material phase, justifying the advantage over the conventional machining process. The SEM analysis also shows that the inner and outer diameters of the stepped circular holes have a direct relationship with the feed rate (f_2) and feed rate (f_1).

Overcut analysis

The SEM images of the machined hole fabricated through the developed hybrid ECM setup are shown in Fig. 6. The holes were generated at different machining conditions mentioned in Table 4. From Fig. 7, the volcanic features with distinct craters were observed across the machined surface. The SEM analysis shows that at higher values of voltage and feed rates, the overcut decreases linearly. The reason for this is that higher voltage and feed rate values effectively regulate the material removal phenomenon. For the first experimental trial as per Table 4, the workpiece provides initial inertial resistance during machining, which results in the generation of higher overcut, as seen in the SEM image of overcut. Thus, an increase in voltage and feed rate values has an inverse relationship with overcut.

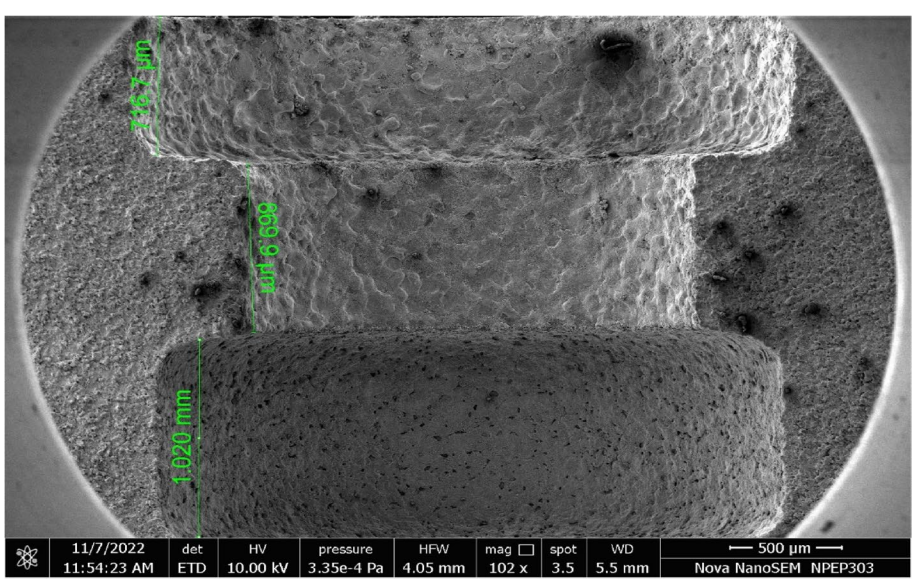

Fig. 7 SEM image for square hole profile with dimensions

Conclusions

This investigation for the stepped circular hole uses ultrasonic-assisted ECM to determine the best machining conditions for the plane circular hole. SEM analysis confirmed the approach's efficacy. It was a two-step study. The multi-objective optimization of a circular hole in a plane was found using ANOVA and TOPSIS in the first step. Stepped hole machining factors are updated using screening experiments. The TOPSIS method was used to optimize the determined factors for stepped hole machining. This study evaluates TOPSIS's applicability in various situations. The following conclusions are drawn from the experimental study and analysis:

- The best experimental run combinations, for plane circular hole machining were 22-21-16-11-12-17-6-7-23-1-13-18-8-2-3-4-14-19-9-24-25-5-15-10-20, whereas experiment 22 was discovered to be the best-performing experiment. The Taguchi analysis of the TOPSIS method for the plane circular hole was analyzed, and experimental results for TOPSIS methods were found to be more satisfactory than the Taguchi analysis. As a result, final optimal machining conditions for the plane circular hole were determined for experimental run 22, where combinations of the input factors are voltage at 18 V, feed rate at 0.8 mm/min, pulse on time at 50 s, ultrasonic on time at 180 s, and amplitude at 80.
- ANOVA analysis reveals that the voltage, feed rate (f_1), and feed rate (f_2) are the primary causes of the stepped circular holes, which are confirmed by SEM image analysis.
- The experimental study revealed that the voltage (V), feed rate (f_1), and feed rate (f_2) were the factors responsible for the stepped hole machining. TOPSIS analysis was performed on these combinations, and the best combinations of the experimental runs for the stepped hole machining are 5–8-7–4-9–6-1–2-3. The Taguchi analysis was performed for this TOPSIS method, and the results show that the experimental results provided by the TOPSIS methods are more satisfactory than the Taguchi method and thus confirmed optimal machining conditions for the stepped hole machining as the voltage at 18 V, feed rate "f_1" at 0.8 mm/min, and feed rate "f_2" at 1.35 mm/min.
- SEM analysis reveals that during ECM, the electrolyte acts as a major bur removal carrier, resulting in uniform surface properties.

Abbreviations

TOPSIS	Technique for Order Preference by Similarity to Ideal Solution
ANOVA	Analysis of variances
SEM	Scanning electron microscope
ECM	Electrochemical machining
MRR	Material removal rate

Acknowledgements

The authors would like to thank Bharati Vidyapeeth's College of Engineering for providing ECM facility for experimentation.

Authors' contributions

Conceptualization, investigation, methodology, writing—original draft, and writing review and editing done by AP. DJ and DK supervise and administrated the article writing work. Also, DK provided the necessary resources required to complete the article. All authors read and approved the final manuscript.

Funding
The authors received no financial support for the research, authorship, and/or publication of this article.

Availability of data and materials
The datasets used and/or analyzed during the current study are available from the corresponding author on reasonable request.

Declarations

Ethics approval and consent to participate
Not applicable. For the current work, the authors have not conducted any animal or human trials.

Consent for publication
Not applicable. Individual data or information has not been included by the authors for the current work.

Competing interests
The authors declare that they have no competing interests.

Received: 14 November 2023 Accepted: 20 February 2024
Published online: 01 March 2024

References

1. Han JC, Dutta S, Ekkad SV (2000) Gas turbine heat transfer and cooling technology. Taylor & Francis, Inc, New York
2. Bogard DG, Thole KA (2006) Gas turbine film cooling. J Propul Power 22(2):249–270
3. Bunker RS (2005) A review of shaped hole turbine film-cooling technology. J Heat Transfer 127(4):441–453
4. Lu X, Leng Y (2005) Electrochemical micromachining of titanium surfaces for biomedical applications. J Mater Process Technol 169(2):173–178
5. Bhattacharyya B, Malapati M, Munda J (2005) Experimental study on electrochemical micromachining. J Mater Process Technol 169(3):485–492
6. Zhu D, Lei WN, Qu NS, Xu HY (2002) Nanocrystaline electroforming process. CIRP Ann 51(1):173–176
7. Egashira K, Hayashi A, Hirai Y, Yamaguchi K, Ota M (2018) Drilling of microholes using electrochemical machining. Precis Eng 54:338–343
8. Fang X, Qu N, Zhang Y, Xu Z, Zhu D (2014) Improvement of hole exit accuracy in electrochemical drilling by applying a potential difference between an auxiliary electrode and the anode. J Mater Process Technol 214(3):556–564
9. Koyano T, Kunieda M (2013) Micro electrochemical machining using electrostatic induction feeding method. CIRP Ann 62(1):175–178
10. McGeough JA (1974) Principles of electrochemical machining. Chapman & Hall
11. Rajurkar KP, Zhu D, McGeough JA, Kozak J, De Silva A (1999) New developments in electro-chemical machining. CIRP Ann 48(2):567–579
12. Klocke F, Zeis M, Harst S, Klink A, Veselovac D, Baumgärtner M (2013) Modeling and simulation of the electrochemical machining (ECM) material removal process for the manufacture of aero-engine components. Procedia Cirp 8:265–270
13. Klocke F, Zeis M, Klink A (2015) Interdisciplinary modelling of the electrochemical machining process for engine blades. CIRP Ann 64(1):217–220
14. Sargison JE, Oldfield MLG, Guo SM, Lock GD, Rawlinson AJ (2005) Flow visualisation of the external flow from a converging slot-hole film-cooling geometry. Exp Fluids 38:304–318
15. Gritsch M, Schulz A, Wittig S (2000) Film-cooling holes with expanded exits: near-hole heat transfer coefficients. Int J Heat Fluid Flow 21(2):146–155
16. Garg VK (2002) Heat transfer research on gas turbine airfoils at NASA GRC. Int J Heat Fluid Flow 23(2):109–136
17. HAN, J. C., & Dutta, S. (2001) Recent developments in turbine blade internal cooling. Ann N Y Acad Sci 934(1):162–178
18. He S, Tong H, Liu G (2018) Spark assisted chemical engraving (SACE) mechanism on ZrO2 ceramics by analyzing processed products. Ceram Int 44(7):7967–7971
19. Gruner A, Schille J, Loeschner U (2016) Experimental study on micro hole drilling using ultrashort pulse laser radiation. Phys Procedia 83:157–166
20. Burger M, Platz A, Werner E (2007) Manufacturing/post-processing of turbine blisks using precision electrochemical machining (PEM)
21. Zhang H, Di J, Zhou M, Yan Y, Wang R (2015) An investigation on the hole quality during picosecond laser helical drilling of stainless steel 304. Appl Phys A 119:745–752
22. Liu WD, Ao SS, Li Y, Zhao CF, Luo Z, Li Q, Luo T (2016) Elimination of the over cut from a repaired turbine blade tip post-machined by electrochemical machining. J Mater Process Technol 231:27–37
23. Wang R, Dong X, Wang K, Sun X, Fan Z, Duan W (2019) Two-step approach to improving the quality of laser micro-hole drilling on thermal barrier coated nickel base alloys. Opt Lasers Eng 121:406–415
24. Romoli L, Vallini R (2016) Experimental study on the development of a micro-drilling cycle using ultrashort laser pulses. Opt Lasers Eng 78:121–131
25. Jain VK, Chavan A, Kulkarni A (2009) Analysis of contoured holes produced using STED process. Int J Adv Manuf Technol 44:133–148
26. Reddy MS, Jain VK, Lal GK (1988) Tool design for ECM: correction factor method

27. Dutta S, Sarma DK (2022) Multi-objective optimization of μ-EDM parameters for μ-hole drilling on Hastelloy C 276 super alloy using response surface methodology and multi-objective genetic algorithm. CIRP J Manuf Sci Technol 39:115–133
28. Pawar A, Kamble D, Ghorpade RR (2021) Overview on electro-chemical machining of super alloys. Materials Today: Proceedings 46:696–700
29. Ashish Pawar, Dr. Dinesh Kamble (2023) Evaluating the effects of multiple hole profiles on gas turbine blade cooling rate: a computational study. Int J Interactive Design Manuf, Springer.
30. Ashish Pawar, Dinesh Kamble, D. B. Jadhav (2022) Performance evaluation of different hole profiles using 2-D CFD model, Proceedings of 1st International Conference (RAMMML-22), ISBN 9781032441313, CRC Press
31. Gerçekcioğlu E, Albaşkara M (2023) Multi-response optimization of electrical discharge machining of 17–4 PH SS using Taguchi-based grey relational analysis. Arch Metall Mater 68(3):861–868

Publisher's Note

Springer Nature remains neutral with regard to jurisdictional claims in published maps and institutional affiliations.